Interstitial Photodynamic Therapy and Glioblastoma: Light Fractionation Study on a Preclinical Model

Thérapie photodynamique interstitielle et glioblastome : étude préclinique du fractionnement

HA Leroy [1,2], M Vermandel [1], MC Tétard [2], B Leroux [1], CA Maurage [3], A Duhamel, JP Lejeune [1,2], S Mordon [1], N Reyns [1,2]

1. Univ. Lille - Inserm, CHU Lille - U1189 - ONCO-THAI - Image Assisted Laser Therapy for Oncology - F-59000 Lille - France.
2. CHU Lille - Department of Neurosurgery - 59000 Lille.
3. CHU Lille - Department of Neuropathology - 59000 Lille.
4. Univ. Lille - CHU Lille - EA2694 - Department of Biostatistics - 59000 Lille.

Mots clés

- Thérapie photodynamique
- Interstitiel
- Fractionnement
- 5-ALA
- Glioblastome
- Apoptose

Résumé

Introduction : Le glioblastome est une tumeur cérébrale de haut grade, récidivant localement. La thérapie photodynamique (PDT) est un traitement local reposant sur l'activation par la lumière d'un photosensibilisant en présence d'oxygène, formant des réactifs cytotoxiques. Le fractionnement de l'illumination peut améliorer son efficacité en permettant une réoxygénation tissulaire.
Objectifs : Évaluer l'efficacité du fractionnement de l'illumination et rechercher une corrélation radio-histologique en utilisant les séquences IRM de diffusion / perfusion.
Matériels et méthodes : Nous avons greffé des cellules U87 dans le putamen droit de 39 rats immunodéprimés. Après absorption du précurseur photosensibilisant (5-ALA), une fibre optique était introduite dans la tumeur. Les rats ont été randomisés dans 3 groupes : sans illumination, illumination « 2 fractions » et illumination « 5 fractions ». Les effets du traitement ont été évalués par IRM postopératoire à 72h. Les spécimens furent finalement sacrifiés pour étude immunohistologique du cerveau.
Résultats : Nous avons observé une augmentation de la diffusion au niveau du centre tumoral parmi les rats traités, particulièrement dans le groupe « 5 fractions ». La perfusion était diminuée au sein de la zone traitée, d'autant plus dans le groupe « 5 fractions ». L'histologie a confirmé les données de l'IRM, avec une nécrose et une apoptose plus importantes associées à une raréfaction angiogénique dans l'aire de traitement après multi-fractionnement « 5 fractions ». Cependant, nous avons observé un œdème périlésionnel majoré et des signes de néoangiogénèse périphérique après PDT « 5 fractions ».
Conclusion : Le traitement interstitiel multifractionné « 5 fractions » induit une nécrose et une apoptose plus importantes au sein du tissu tumoral mais est également à l'origine d'un œdème majoré et d'une néoangiogénèse périphérique. La diffusion et perfusion en IRM ont permis de prédire les lésions histologiques.

Keywords

- Photodynamic therapy
- Interstitial
- Fractionation
- 5-ALA
- Glioblastoma
- Apoptosis

Abstract

Background: Glioblastoma is a high-grade cerebral tumor with local recurrence and poor outcome. Photodynamic therapy (PDT) is a local treatment based on the light activation of a photosensitizer (PS) in the presence of oxygen to form cytotoxic species. Fractionation of light delivery may enhance treatment efficiency by restoring tissue oxygenation.
Objectives: To evaluate the efficiency of two light fractionation schemes, using immunohistological data.
Materials and Methods: Thirty-nine "Nude" rats were grafted with human U87 cells into the right putamen. After PS precursor intake (5-ALA), an optic fiber was introduced into the tumor. The rats were randomized in three groups: without light, with 2 fractions and 5 fractions. Treatment effects were assessed from brain immunohistology.
Results: Histology confirmed more extensive necrosis and apoptosis associated with a rarified angiogenic network in the treatment area, after multifractionated PDT. However, we observed more surrounding edema and neovascularization in the peripheral ring after 5-fractionned PDT.
Conclusion: Interstitial PDT with fractionated scheme induced specific tumoral lesions. The 5 fractions scheme was more efficient, inducing greater tumoral necrosis and apoptosis, but also significant peripheral edema and neovascularization.

Correspondance :

Dr Maximilien Vermandel
INSERM U1189 - ONCO-THAI - Université de Lille - CHRU de Lille - 1, avenue Oscar Lambret - 59037 Lille Cedex.
Tel : 0033 3 20 44 67 21 - E-mail : m-vermandel@chru-lille.fr

Disponible en ligne sur www.academie-chirurgie.fr

DOI : 10.14607/emem.2016.1.011

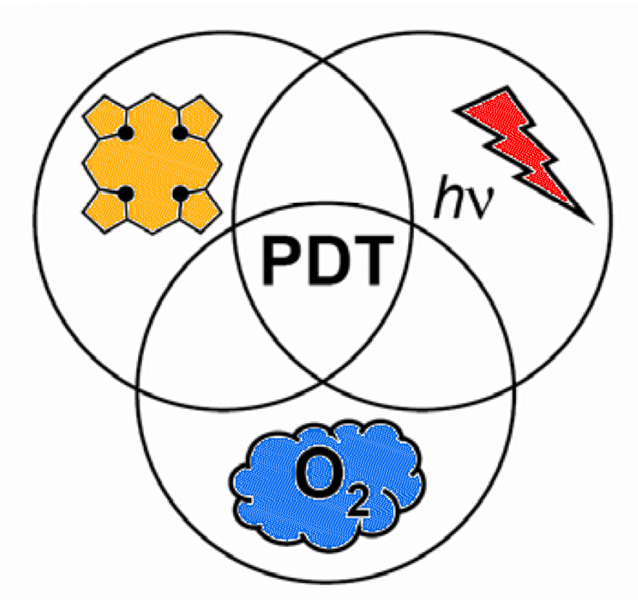

Figure 1. PDT effects rely on the simultaneous presence of a photosensitizer, light using an optic fiber and the presence of oxygen.

The incidence of high-grade gliomas is constantly increasing over the last decades, reaching an incidence superior to 5 per 100,000 population and leading to 3% of all cancer deaths for patients aged 35 to 64 years-old (19). Glioblastoma multiforme (GBM) is the most infiltrative and aggressive primitive cerebral tumour (grade IV, WHO). Despite the armamentarium, relying on maximal microsurgical resection followed by a concomitant radio-chemotherapy, patients harboring GBM still experience dismal prognosis with a median survival of 15 months (12,20). Due to the invasive character of high-grade gliomas, GBM recurrence occurs in most of 85% in the 2.5 cm of the initial operative cavity (22). The key point is to improve local control of the disease. In this context, photodynamic therapy (PDT), using 5-Aminolevulinic acid (5-ALA) (1) or talaporfin sodium (17) induced fluorescence, has a role to play. Recent studies reported a significant overall survival increase in patients treated with interstitial PDT, up to 4 years (2,26). Interstitial PDT consists in introducing optic fibers directly through the tumor without craniotomy. This technique is particularly relevant for non-operable tumor such as insular GBM or for elderly patients. 5-ALA PDT is a non-thermic technology, based on the synergy of three elements: a photosensitizer (5-ALA), lighting at a precise wavelength and the presence of oxygen (Fig 1).

5-ALA is a second-generation photosensitizer (PS) precursor already used in clinical practice for fluorescence-guided resection since 2007 in Europe (9,23,27). 5-ALA is a natural prodrug produced in all human cells mitochondrias with the exception of erythroblasts, which contain no mitochondria (13). 5-ALA is highly selective substance for tumoral tissue, has a good oral bioavailability and presents a shorter skin photosensitization period in comparison with previous PS (30). Going through several enzymatic modifications taking part in the haem biosynthesis, and after a final oxidation step, 5-ALA is transformed into protoporphyrin IX (PpIX). PpIX is a photoactive compound (the real second generation precursor) which absorption peak of light is near 635 nm. Following such an excitation, two types of reactions are occurring:

1) production of free radicals;
2) oxidative species formation (11). In both case the presence of oxygen is needed to generate such photodynamic interactions. As a matter of fact, treatment delivery has to take into account the specific tissue oxygen pressure in order to increase therapeutic effects (6). The fractionation of the lighting has been proposed to answer this issue (7). During “off” periods, the tissue oxygen pressure has been reported to increase, allowing repetitive efficient light exposures (7). Light fractionation is supposed to enhance photodynamic efficiency without complicating treatment delivery.

Our main hypothesis was that light fractionation is able to enhance the therapeutic effects of PDT. Our study aimed at evaluating the effects with immunohistological analysis on a preclinical model of GBM.

Materials and methods

The main objective of our study was to evaluate the effects of two distinct light deliveries:

1) 2-fractionated lighting; and
2) 5-fractionated lighting. These two groups were compared to a SHAM group with no light delivery.

Preclinical model

Ethical considerations

All operative procedures and animal care were performed in line with the French Government’s guidelines (decree 2001-464, 29 may 2001) and with the Laboratory Animal Care and Use Committee. Our institutional ethic review board approved the study protocol (N°01878.01).

Animals

Specimens were nude rats which phenotype was Fox n1 rnu/rnu obtained from Charles River©. These partially immunocompromised rats were elected to tolerate such a xenograft. A quarantine period of 10 days from their reception was observed before performing the GBM cells graft. Grafted rats were aged of 8 weeks and weighted around 150 g.

Cells

We used human GBM cells U87. Cells coming from the American type culture collection (ATCC HTB-14) were preserved at -80°C. After defrosting, they were cultured as an adherent monolayer in DMEM, complemented with 10% foetal bovine serum, 100 units/ml penicillin, 100 µg/ml streptomycin, GlutaMAX™ (cell culture media including L-glutamine, L-alanyl-L-glutamine), sodium pyruvate, additional L-serine, and L-asparagine. First cultures benefited from additional growing factors to enhance cell multiplications. Cells incubated in a 5% CO2 atmosphere at 37°C. When a sufficiently high concentration was reached in the culture media, U87 cells were rinsed with phosphate buffered saline solution. When detached by trypsination, U87 cells were suspended again in DMEM to obtain a concentration of 10^5 cells/µL.

Surgical grafting procedure

U87 grafts were performed in stereotactic conditions, allowing a high precision and reproducibility. For anesthetic induction, a mask was used to deliver isoflurane (4-5%) inhalation mixed with oxygen (1L/min). During the whole procedure, sedation was maintained by a continuous isoflurane inhalation between 2 and 4%, depending on cardiac and respiratory frequencies monitoring. We used a stereotactic frame (900M, ULTEM-1000, Nylon 6-6 and Delrin, Kopf®, USA) allowing micrometric precision. The head of the rat was maintained at the center of the frame with to two ear bars (scale on the bars) perpendicular to the anteroposterior axis. The tooth bar fixed the plane of the head. An arm connected to the frame slide and the micromanipulator that could be moved in three planes of space (x, y, z) with three-micrometer screws. Once the rat attached to the stereotactic device, local anesthesia with subcutaneous injection of 1 mL of 2% lidocaine was performed after skin disinfection. A midline incision of the scalp was performed and an orthostatic retractor was set up to discover the bone. The operative area was rinsed with saline and buffered with sterile gauze to visualize cranial sutures including bregma and lambda. The horizontality of the head was controlled by measuring the dorso-ventral coordinates of bregma and lambda points with, if necessary, adjusting the positioning of the head. According to the Atlas of Paxinos and Watson (21), the stereotactic coordinates of the graft site to the bregma (zero point coordinates) were calculated for implantation at the right caudal putamen. Then, a single burr-hole craniotomy with a 1 mm drill diameter was performed. A patented cranial anchor (Publication N°WO2012176050), developed in partnership with the University of Lorraine, France, was then fixed using a biological glue (Dermabond, Ethicon). This MRI compatible anchor allowed grafting U87 cells in orthotopic conditions and subsequently permitted to set in the same site the optic fiber delivering PDT. Once the cranial anchor firmly stuck, we proceeded with the implementation of the nanoliter syringe pump fixed on the stereotaxic apparatus (KDS-310, Kdscientific, Holliston MA, USA). Then we slowly introduced the 30G needle of a Hamilton syringe containing 7 µL of U87 cells suspension through the cannula of the anchor. Once in the putamen, the needle was left in place during 15 min before the start of the injection to allow the brain tissue to comply with the needle and prevent reflux. The cells were injected over a period of 10 minutes, at an injection speed of 0.5 µL/min to deliver a total injected volume of 5 µL containing 5 x 10^5 U87 cells. After injection, the needle was left in place 15 minutes more before being gradually removed to avoid the rise of injected cells upon removal of the syringe needle. A cap was then placed on the cannula of the anchor. Eventually, skin edges were sutured with Vicryl 4/0 (Ethicon, USA) taking care not to cover the hole of the anchor. The rat was identified and placed alone in a Plexiglas cage and monitored until waking-up.

Imaging

A 7 Tesla MRI was used to perform brain imaging on rats (Bruker, Biospec, Ettlingen, Germany). Treatment decision was taken when the tumour graft on MRI had a maximum coronal diameter superior to 2 mm. Two types of antenna were used. A surface antenna placed over the scalp of the animal for signal reception was used to assess tumor's growth. For image-guided procedures, a transceiver cylindrical antenna of 72 mm internal diameter was used to assess the fiber positioning. Sedation protocol was the same that for surgery.
MRI analyses were carried out 7 days after the U87 graft to check the quality and the extent of engraftment. Then MRI was repeated during the treatment. A T2-weighted TurboRARE sequence (24) was systematically performed in the axial plane to characterize the geometry and the position of the glial tumor. A T1-weighted sequence was performed routinely before and after gadolinium injection on the axial plane using a type of spin echo RARE (32).

Treatment

Interstitial photodynamic therapy (iPDT) delivering

At least 4h prior to the treatment, the photosensitizer precursor (5-ALA) was administered intraperitoneally at a dose of 100 mg/kg (18). All rats, regardless of their group received 5-ALA injection. During this period, animals were kept away from direct light exposure to prevent skin reaction, such as erythema or burn, until 5-ALA elimination after 72h. Before lighting, the rats were anesthetized as previously described and placed on the MRI table. A first MRI sequence (T2 and / or

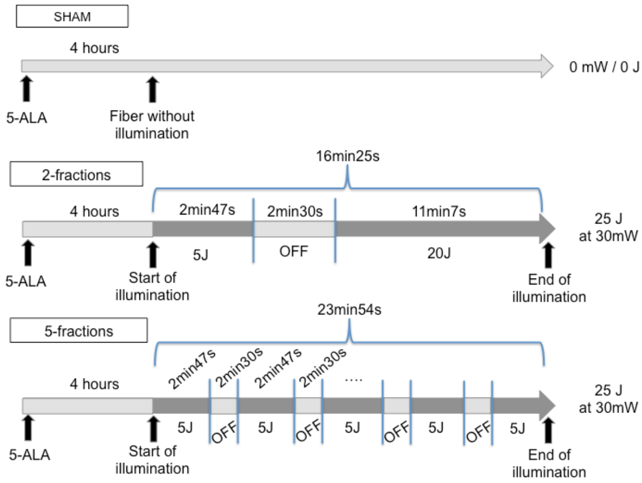

Figure 2. Description of lighting schemes for each group, SHAM, 2 fractions, 5 fractions. The total energy delivered dose was 25 J at a high power of 30 mW (measured at the fiber tip).

T1) was performed to calculate the depth to which the fiber was to be introduced to achieve the higher third of the tumour. A silica optic fiber Ultrasil 272 ULS (OFS, Norcross, USA) of 350 µm outside diameter having a numerical aperture of 0.29 was then inserted into the brain through the cannula of the anchor, at the predetermined depth. MRI acquisition (T1) controlled the positioning of the fiber before starting enlightenment. Light from a laser diode 635 nm could then be issued interstitially via the introduced optic fiber. According to the randomized groups: SHAM, 2 fractions or 5 fractions, the appropriate lighting scheme was delivered (Fig 2). Light pattern in terms of irradiance and fractionation duration were based on the work of Curnow et al and the results of Tétard et al (6,29,28).
For the SHAM group, the fiber was put in place without enlightenment. We opted for this type of control group to take into account any morbidity or mortality induced by the 5-ALA intraperitoneal injection or the optic fiber positioning that may impact on the MRI and immunohistological data. For the 2 fractions group, lighting began with a fraction of 5 J delivered over 2 min 47 s, followed by a pause of 150 s. Then the 20 J remaining were delivered on 11 min 7 s. The 5 fractions group received 5 fractions of 5 J each, all separated by an interval of 150 s. Thus the two treated groups received a total energy of 25 J at with a power of 30 mW at the tip of the optic fiber.
At the end of treatment, the fiber was removed and the cap covering the anchor repositioned. The animal was placed alone in his cage and monitored until the resumption of physiological activity and kept away from light for 24 h to prevent photosensitivity skin reaction. Every single rat benefited from post-operative intraperitoneal corticosteroids injection, which consisted in 1 mg/kg of methylprednisolone, in prevention of iPDT induced edema.

Post treatment follow-up

Daily clinical monitoring, including a measure of weight, could detect any complication due to the operation or treatment and could evaluate the behavior of animals. The animals were sacrificed by exsanguination under general anesthesia 72h after iPDT. Euthanasia was earlier in case of signs of neurological pains.

Immunohistological analysis

The brains were removed immediately upon the sacrifice and immersed in formalin (10%, 0.9% NaCl). Hematoxylin and eosin standard staining was performed on slides from paraffin

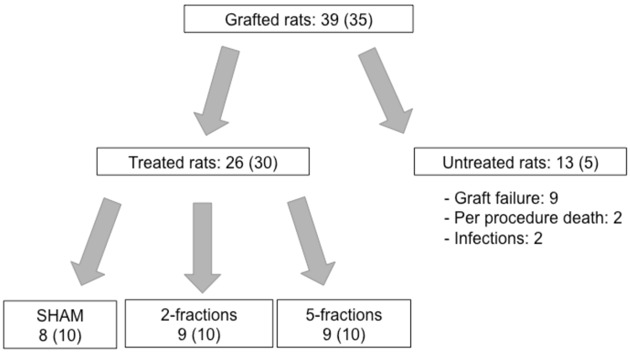

Figure 3. Study flowchart. Theoretical calculated numbers of samples appear in brackets.

blocks. The following parameters were particularly studied and quantified:

- Necrosis
- Inflammation / edema
- Macrophage infiltrate
- Neoangiogenesis
- Demyelinating lesions

Specific apoptosis analyses were performed by immunohistochemistry using the TUNEL method (Apoptag® Plus Peroxidase In Situ, Millipore, USA). We stratified the importance of apoptosis in three groups: physiological number of apoptotic structures for the studied tissue, number increased slightly compared to the physiological level, and number significantly increased. A senior neuropathologist reviewed all slides.

Statistical analysis

The number of subjects required was estimated to obtain a statistical power of 80%, α = 5%. However, given the preliminary nature of this study, we did not have available literature data for approaching the minimum difference of interest or the variance for the tested parameters. We used as references other preclinical studies in rats to clarify the sample size, taking into account 10-15% loss (3). Ideally, we wanted to achieve more than 10 animals per group. For treatment allocation, we performed randomization in blocks of 6 to balance the size of each of the 3 groups, SHAM, 2 fractions and 5 fractions.

Continuous data were presented with their mean and standard deviation (σ) or median and interquartile range (IQR) (e.g. volume measurements median). In front of small samples, non -parametric test were conducted. To test the symmetry of distribution among samples, Wilcoxon Rank Sum test was performed. For comparison tests between more than two independent groups, we used the Kruskal-Wallis test. To compare independent groups with ordered alternatives, the Jonckheere-Tepstra trend test was done (e.g. diffusion gradient or perfusion according to the allocated treatment). To compare the histological findings, considering small numbers (theoretical groups < 5) we performed Fisher exact test. Data were analyzed with SAS software version 9.3 (SAS Institute, Cary, NC).

Results

We performed transplants in 39 rats. Twelve rats benefited from a second graft procedure after failure of the first. The mean duration of graft operation was 2 h. Among them, 26 specimens developed sufficiently large tumors to be treated. The rate of satisfactory graft reached 51%. The transplant procedure was well tolerated by the majority of rats. We reported 2 deaths related to an Isoflurane overdose during anesthesia that caused cardiorespiratory arrest. Two additional rats harbored a surgical site infection. They had to be sacrificed earlier. The median time before the tumor reached a size compatible with iPDT was 15 days (IQR, 11-22). The mean tumor volume measured on MRI was 4.7 mm^3 (σ = 2.86). The mean treated volume did not differ significantly between the 3 groups, SHAM, monofractionated and multifractionated (p = 0.44).

After randomization of the 26 rats immediately before treatment, we obtained 8 rats in the SHAM group, 9 in the 2 fractions group and 9 in the 5 fractions group (Fig 3).

Anatomopathology

19 tumors slides with HE staining over the 24 treated rats were studied (Table 1). Indeed, 5 slides could not be interpreted because of aliasing artifacts or incorrectly fixed tissue. The extent of necrosis was significantly greater among the treated group compared to the SHAM group (p < 0.001). We observed a more extensive necrosis in the 5 fractions group in comparison with the 2 fractions group, without statistical difference (p = 0.47). The necrosis induced by PDT resulted in dissociation between the tumor and the adjacent parenchyma. In the necrotic area, no more vascular structures were observed. However, in the periphery of the treated area, we noticed a higher vascular density (p = 0.017) (Fig 4). These likely new vessels were found more frequently in the 5 fractions group (p = 0.028). The peritumoral edema was also more extensive in the treated groups (p = 0.009), but with no difference between the 2 fractions or the 5 fractions group. A major macrophagic infiltration was associated to this edema among treated rats (p = 0.006). In several treated rats, we observed some vacuolated structures corresponding to demyelination injuries (Fig 4).

	Necrosis		Peripheral Neovascularization		Peripheral Edema		Macrophagic infiltration	
	Yes	No	Yes	No	Yes	No	Yes	No
SHAM	0	7	0	7	2	5	1	6
2-FRACTIONS	5	2	2	5	6	1	5	2
5-FRACTIONS	5	0	5	0	5	0	5	0

Table 1. Histological experiments summary.

Table 2. Distribution of the treated rats with immuno-histological analyses of apoptosis. A significant difference was reported between the three groups (p = 0.001) with an increase of the apoptotic labelling in the 5 fractions group (p = 0.005).

	Apoptosis		
	No Increase	Slight Increase	Important Increase
SHAM	4	0	0
2-FRACTIONS	2	6	0
5-FRACTIONS	0	2	5
TOTAL	**6**	**8**	**5**

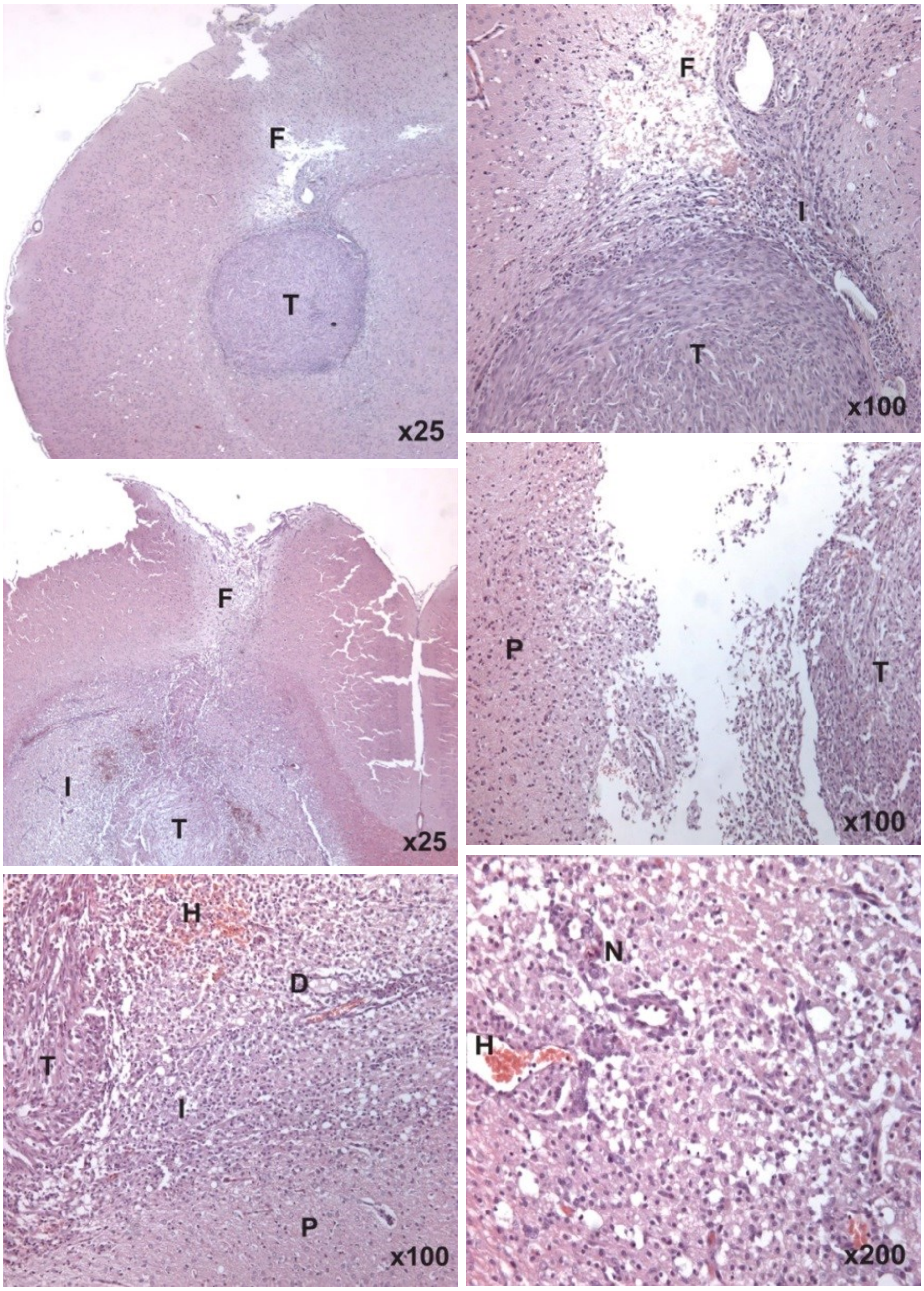

Figure 4.
(a): low magnification, tumor of a rat belonging to the SHAM group, T: unaltered tumor, F: path of the optical fiber.
(b): higher magnification of the upper pole of the same tumor, T: compact tumor with “mesenchymal like” glial cells, I: slight inflammation surrounding the tumor, close to the passage of the fiber, F: path of the fiber.
(c): treated tumor in 5 fractions group, T: dissociated tumor of the parenchyma following PDT, fragmented appearance, I: major circumferential post-processing inflammation with many macrophages.
(d): same tumor at a higher magnification, cleavage plane between the tumor tissue (T) and the healthy parenchyma (P).
(e): same tumor, zoom on the periphery, T: tumor, I: inflammation and macrophagic infiltration, H: red blood cells with new vessels, P: healthy parenchyma with no infiltration, D: demyelinating lesions appearing in the form of vacuoles.
(f): new vessels in high magnification

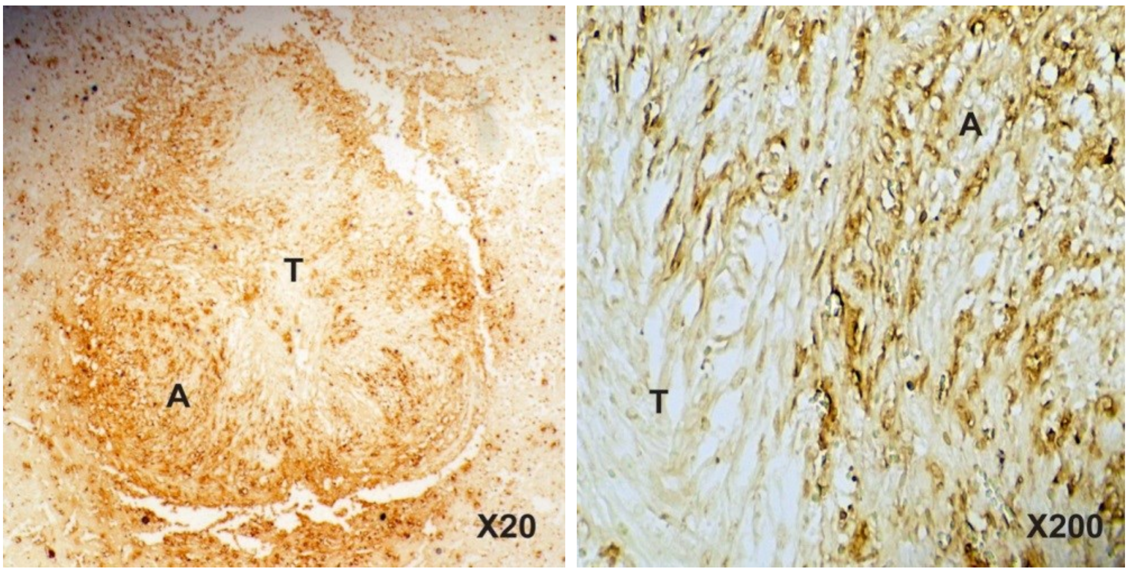

Figure 5. Slide with immunostaining of apoptosis from a rat belonging to the multifractionated group.
(a): low magnification, T: tumor “pear-shaped”, A: numerous apoptotic bodies in brown, predominantly spread in the periphery of the treated area.
(b): higher magnification, T: “mesenchymal like” tumor cells, A: apoptotic bodies in the periphery.

Immunolabelling of apoptosis

19 slides with specific immuno-labeled antibodies of apoptosis were studied (Table 2, Fig 5). No increase of the apoptotic marker in the SHAM group was observed in comparison with the positive control slide. Among the 2 fractions group, an increase of apoptosis in 6 out of 8 rats was noticed. In the 5 fractions group, an increase of the apoptotic marker in 7 rats out of 7 was observed. Benchmarking reported a statistically significant difference between the 3 groups ($p = 0.001$). Comparing the 2 fractions and the 5 fractions groups, significant increase in the marking of apoptosis in the 5 fractions group ($p = 0.005$) was observed.

Discussion

Our main objective was to study the effects of the fractionation of light using PDT in terms of damage induced to the treated tumor.
The use of human glioblastoma U87 cells constitutes a validated preclinical model of glioblastoma according to present literature (10,31). This cell line allows rapid tumor growth and a relatively constant engraftment rate (29). Nevertheless, U87 does not reproduce all pathological aspects of human glioblastoma. They are less invasive and present no spontaneous tumor necrosis. However, the lack of such spontaneous necrosis allowed us to assign post-treatment necrosis to the PDT itself, ensuring a high intrinsic accountability. For further experiments, we should expand the cell cultures to include low passage primary xenografts, as well as cell lines that have defined genetic mutations.
The administration of interstitial PDT was responsible for an increase of peritumoral edema compared to the SHAM group ($p < 0.01$). The volume of peripheral edema averaged 25 mm^3, which represented a large volume in comparison with the average 4.7 mm^3 treated tumor volume. Delivering 5 fractioned lights tended to produce a volume of edema larger than two fractions lighting.
Histological study described a more extensive necrosis among the treated group compared to the SHAM group ($p = 0.008$). Tumors induced by U87 cells grafts do not develop spontaneous necrosis (3). Post-PDT necrosis can then be directly attributable to the treatment itself. Interstitial PDT produced necrosis, especially since we delivered fractionated lighting. The extent of necrosis appeared increased in the 5 fractions group compared to the 2 fractions group, but without statistical difference. Necrosis, found as dissociation from healthy parenchyma, stood at the immediate periphery of the firing of the optical fiber, over few millimeters, which corresponds to the literature data (29). Necrosis is the majority death pathway induced by PDT (5). Within necrotic areas, it was no longer observed vascular structures. However, we described in the periphery of the treated area a resurgence of new vessels among some specimens belonging to the multifractionated group ($p = 0.028$). The onset of neovascularization was explained in part by the resulting hypoxia during PDT and by the induced expression of VEGF (34). Some teams propose therefore to combine PDT with the use of antiangiogenic molecules to increase overall survival in specimens (14).
The administration of interstitial PDT was responsible for greater peritumoral edema compared to the SHAM group ($p = 0.027$). The edema results from the dysregulation of transepithelial ions transport and lesion of tight junctions of the vascular walls induced by PDT, causing vasogenic edema (35). Peripheral edema has been described as the main pitfall of PDT (8,33). Nevertheless, administration of corticosteroids intraperitoneally to all rats helped to ensure good tolerance of the procedure. Post-PDT follow-up was uneventful until sacrifice. Only 2 rats of 26 died within the 72 hours interval after PDT, because of cerebral herniation or hydrocephalus. These 2 specimens harbored larger tumour volume with a midline deviation at the treatment time. This could be a contraindication of PDT in future studies.
Significant macrophagic infiltration was also displayed among the treated rats ($p = 0.008$). Interstitial PDT is known to induce a strong activation of the immune system, initially via innate immunity associated with local inflammation before to stake adaptive immunity (4,16). Finally, in several treated rats, we observed rare demyelinating lesions in the periphery of the area concerned by the light (Fig 4). This fact reminds that although PDT is recognized as a selective treatment, adjacent healthy parenchyma can be damaged, in particular neurons (8).
About immunohistological study of apoptosis, we reported a significant difference between the three groups, SHAM, 2 fractions and 5 fractions groups ($p = 0.001$). Interstitial PDT induces the apoptosis of U87 cells by inhibiting the survival factors (decreasing the nuclear factor kappa) and activating caspase-dependent pathways (15). Furthermore, the highest degree of apoptosis was found among specimens belonging to the 5 fractions group ($p = 0.005$) (15). This data is in line with previous studies reporting a higher level of apoptosis when the light was delivered over a long period of time (28). The “metronomic” administration of the light, i.e. at low irradiance over a longer period, appears to further increase the level of apoptosis in the tumour tissue (25). It will be the subject of a future study.

Conclusion

Fractionated interstitial 5-ALA PDT induced targeted tumor lesions. Major significant effects were necrosis, apoptosis, and reduced central tumor vascularization. This treatment modality also encouraged the involvement of the host immune system.
Five fractions treatment has provided improved efficiency in terms of tumor destruction, resulting in more cell deaths by apoptosis in comparison with the 2 fractions treatment. However, this modality was associated with a more important post -treatment perilesional edema that should be prevented by corticosteroids.

Conflict of interest

None.

References

1. Angell-Petersen E, Spetalen S, Madsen SJ, Sun CH, Peng Q, Carper SW, et al. Influence of light fluence rate on the effects of photodynamic therapy in an orthotopic rat glioma model. J Neurosurg 2006;104:109-17.
2. Beck TJ, Kreth FW, Beyer W, Mehrkens JH, Obermeier A, Stepp H, et al. Interstitial photodynamic therapy of nonresectable malignant glioma recurrences using 5-aminolevulinic acid induced protoporphyrin IX. Lasers in surgery and medicine 2007;39:386-93.
3. Candolfi M, Curtin JF, Nichols WS, Muhammad AG, King GD, Pluhar GE, et al. Intracranial glioblastoma models in preclinical neuro-oncology: neuropathological characterization and tumor progression. J Neuro-oncol 2007;85:133-48.
4. Cecic I, Stott B, Korbelik M. Acute phase response-associated systemic neutrophil mobilization in mice bearing tumors treated by photodynamic therapy. International immunopharmacology 2006;6:1259-66.
5. Coupienne I, Fettweis G, Rubio N, Agostinis P, Piette J. 5-ALA-PDT induces RIP3-dependent necrosis in glioblastoma. Photochem Photobiol Sci. 2011;10:1868-78.
6. Curnow A, Haller JC, Bown SG. Oxygen monitoring during 5-aminolaevulinic acid induced photodynamic therapy in normal rat colon: comparison of continuous and fractionated light regimes. Photochem Photobiol Sci. 2000;58:149-55.

7. Curnow A, McIlroy BW, Postle-Hacon MJ, MacRobert AJ, Bown SG. Light dose fractionation to enhance photodynamic therapy using 5-aminolevulinic acid in the normal rat colon. Photochem Photobiol Sci. 1999;69:71-6.
8. Dereski MO, Chopp M, Chen Q, Hetzel FW. Normal brain tissue response to photodynamic therapy: histology, vascular permeability and specific gravity. Photochem Photobiol Sci. 1989;50:653-7.
9. EuropeanMedicinesAgency Gliolan Scientific Discussion, 2007.
10. Han S, Li Z, Master LM, Master ZW, Wu A. Exogenous IGFBP-2 promotes proliferation, invasion, and chemoresistance to temozolomide in glioma cells via the integrin Œ≤1-ERK pathway. Br J Cancer, 2014;111:1400-9.
11. Henderson BW, Dougherty TJ. How does photodynamic therapy work? Photochem Photobiol Sci. 1992;55:145-57.
12. Iacob G, Dinca EB. Current data and strategy in glioblastoma multiforme. J Med and life 2009;2:386-93.
13. Ishizuka M, Abe F, Sano Y, Takahashi K, Inoue K, Nakajima M, et al. Novel development of 5-aminolevurinic acid (ALA) in cancer diagnoses and therapy. International immunopharmacol 2011;11:358-65.
14. Jiang F, Zhang X, Kalkanis SN, Zhang Z, Yang H, Katakowski M, et al. Combination therapy with antiangiogenic treatment and photodynamic therapy for the nude mouse bearing U87 glioblastoma. Photochemistry and photobiology 2008;84:128-37.
15. Karmakar S, Banik NL, Patel SJ, Ray SK. 5-Aminolevulinic acid-based photodynamic therapy suppressed survival factors and activated proteases for apoptosis in human glioblastoma U87MG cells. Neuroscience letters. 2007;415:242-7.
16. Korbelik M. PDT-associated host response and its role in the therapy outcome. Lasers in surgery and medicine. 2006;38:500-8.
17. Muragaki Y, Akimoto J, Maruyama T, Iseki H, Ikuta S, Nitta M, et al. Phase II clinical study on intraoperative photodynamic therapy with talaporfin sodium and semiconductor laser in patients with malignant brain tumors. J Neurosurg. 2013;119:845-52.
18. Olzowy B, Hundt CS, Stocker S, Bise K, Reulen HJ, Stummer W. Photoirradiation therapy of experimental malignant glioma with 5-aminolevulinic acid. Journal of neurosurgery. 2002;97:970-6.
19. Omuro A, DeAngelis LM. Glioblastoma and other malignant gliomas: a clinical review. JAMA. 2013;310:1842-50.
20. Ostrom QT, Bauchet L, Davis FG, Deltour I, Fisher JL, Langer CE, et al. The epidemiology of glioma in adults: a "state of the science" review. Neuro-oncology. 2014;16:896-913.
21. Paxinos G, Watson C, Pennisi M, Topple A. Bregma, lambda and the interaural midpoint in stereotaxic surgery with rats of different sex, strain and weight. Journal of neuroscience methods. 1985;13:139-43.
22. Petrecca K, Guiot MC, Panet-Raymond V, Souhami L. Failure pattern following complete resection plus radiotherapy and temozolomide is at the resection margin in patients with glioblastoma. Journal of neuro-oncology. 2013;111:19-23.
23. Sanai N, Snyder LA, Honea NJ, Coons SW, Eschbacher JM, Smith KA, et al. Intraoperative confocal microscopy in the visualization of 5-aminolevulinic acid fluorescence in low-grade gliomas. J Neurosurg. 2011;115:740-8.
24. Schuierer G, Reimer P, Allkemper T, Peters PE. Fast and ultrafast MRI of the brain. Radiologe. 1995;35:894-901.
25. Singh G, Alqawi O, Espiritu M. Metronomic PDT and cell death pathways. Methods in molecular biology (Clifton, NJ). 2010;635:65-78.
26. Stummer W, Beck T, Beyer W, Mehrkens JH, Obermeier A, Etminan N, et al. Long-sustaining response in a patient with non-resectable, distant recurrence of glioblastoma multiforme treated by interstitial photodynamic therapy using 5-ALA: case report. Journal of neuro-oncology. 2008;87:103-9.
27. Stummer W, Tonn JC, Mehdorn HM, Nestler U, Franz K, Goetz C, et al. Counterbalancing risks and gains from extended resections in malignant glioma surgery: a supplemental analysis from the randomized 5-aminolevulinic acid glioma resection study. Clinical article. J Neurosurg. 2011;114:613-23.
28. Tetard MC, Reyns N, Leroy HA, Lejeune JP, Mordon S, Vermandel M. Light Dose Fractionation to Enhance Photodynamic Therapy With 5-Aminolevulinic Acid in Human glioma xenografts, in The International Congress on Photodynamic Applications (ICPA 2014) Dundee, Scotland. 2014.
29. Tetard MC, Vermandel M, Mordon S, Lejeune JP, Reyns N. Experimental use of photodynamic therapy in high grade gliomas: a review focused on 5-aminolevulinic acid. Photodiagnosis Photodyn Ther. 2014;11:319-30.
30. Webber J, Kessel D, Fromm D. Side effects and photosensitization of human tissues after aminolevulinic acid. The Journal of surgical research. 1997;68:31-7.
31. Wicks RT, Azadi J, Mangraviti A, Zhang I, Hwang L, Joshi A, et al. Local delivery of cancer-cell glycolytic inhibitors in high-grade glioma. Neuro-oncology. 2015;17:70-80.
32. Wong EC, Buxton RB, Frank LR. Implementation of quantitative perfusion imaging techniques for functional brain mapping using pulsed arterial spin labeling. NMR in biomedicine. 1997;10:237-49.
33. Yoshida Y, Dereski MO, Garcia JH, Hetzel FW, Chopp M. Neuronal injury after photoactivation of photofrin II. The American journal of pathology. 1992;141:989-97.
34. Zhan Q, Yue W, Hu S. Effect of photodynamic therapy and endostatin on human glioma xenografts in nude mice. Photodiagnosis and photodynamic therapy. 2011;8:314-20.
35. Zhang X, Cong D, Shen D, Gao X, Chen L, Hu S. The effect of bumetanide on photodynamic therapy-induced peri-tumor edema of C6 glioma xenografts. Lasers in surgery and medicine. 2014;46:422-30.